DIGITAL SLIDING MODE CONTROLLED THREE-PHASE BOOST INVERTER IMPLEMENTED IN DSC TMS320F2812

Marcello Mezaroba[1], Priscila dos Santos Garcia Giacomini[1], Antonio Heronaldo de Sousa[1] and Luiz Carlos de Souza Marques[2]
1 - Santa Catarina State University – UDESC
Mail Box 631, Zip Code: 89.223-100, Joinville, SC, Brazil
mezaroba@joinville.udesc.br, priscila@joinville.udesc.br, heron@joinville.udesc.br
2 – Santa Maria Federal University – UFSM.
Av. Roraima Nº 1000, Camobi. Zip Code: 97105-900 - Santa Maria - RS – Brazil
marques_lcsm@hotmail.com

***Abstract* – This paper presents a Digital Sliding Mode Controlled Three Phase Boost Inverter. The main usage of this converter is to provide the necessary AC voltage to a three-phase induction motor from batteries. The sliding mode control, which is a hysteresis based control methodology, was implemented using a TMF320F2812 Digital Signal Controller (DSC).**

The theoretical analysis, basic equations and the design methodology is presented in this work. The converter's main advantages are only one stage to boost and invert the battery energy and small number of components.

***Keywords* – DC-AC Converter, Sliding Mode, Three-Phase Boost Inverter.**

I. INTRODUCTION

In the industry, the direct current (DC) machines have largely lost their popularity in the last years to the alternate current (AC) ones. There are clear preferences for induction machines due to low maintenance, durability and reduced costs.

However, in certain applications, it is not so easy to replace DC machines, like Automatically Guided Vehicles (AGV) and electrical fork lift trucks, used in great part of the industrial environment.

Currently, one of the AGV's problems is the low autonomy of its batteries and the usage of specials machines and converters, which usually have high costs and are difficult to be found.

The topology presented in this paper is an alternative for this vehicles, it is worth noting this topology invert and boost the energy using a single stage, allowing the usage of commons AC machines.

In Fig. 1 is shown the classic topology and Fig. 2 the alternative topology for the AGV's.

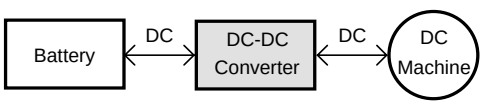

Fig. 1 Classic Power Topology of the AGV

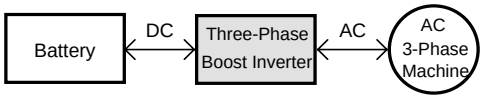

Fig. 2 Alternative Topology of the AGV

To solve the problem about AGV's autonomy, many technical works had been developed. One of those works was a regenerative step-up/step-down DC-DC ZVS PWM converter with active clamping [1]. This converter has the advantage to boost the input voltage to a high output voltage, but it is a DC-DC converter, what mean it is necessary a DC machine or another stage to invert the output voltage.

The converter presented in this paper has just one stage to boost and invert the output voltage. Many control techniques have been proposed and analyzed to the boost inverter. Among them, there is one based on control techniques derived from variable structure system (VSS) theory, like Sliding Mode (SM) control [2-4].

In [5] it is presented a general purpose sliding mode control for DC-DC converter application. In this article, it was introduced a tutorial on how to calculate the sliding mode parameters and presented examples for Cuk and Sepic converters.

The sliding mode controller for the Boost Inverter is presented in [6-8]. Those implementations had good results but there are some differences between that technique and the one implemented in this article. The main difference is the control previously were analog and implemented in a single phase boost inverter and this one is digitally controlled using the DSC (Digital Signal Controller) TMS320F2812 from *Texas Instruments* implemented in a three-phase boost inverter.

II. PRESENTATION OF THE CIRCUIT

The three-phase boost inverter consists of three current reversible power converters associated. The power converter used in this work has the same switches number as a regular inverter, with the addition of the input inductors that are necessary to step-up the input voltage.

The power topology is presented in Fig. 3 and the output phase voltages and line voltages waveforms of this converter can be observed in Fig. 4.

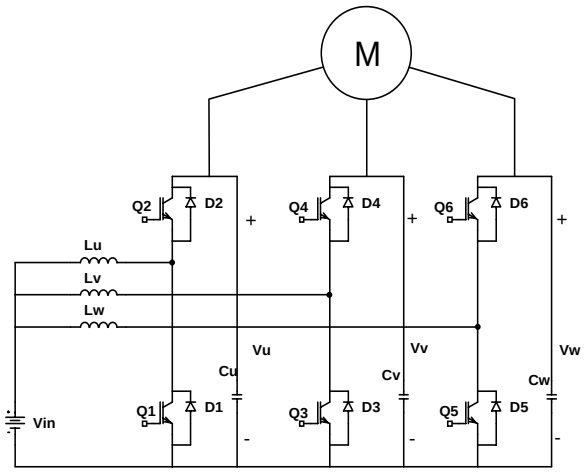

Fig. 3 Three - Phase Boost Inverter

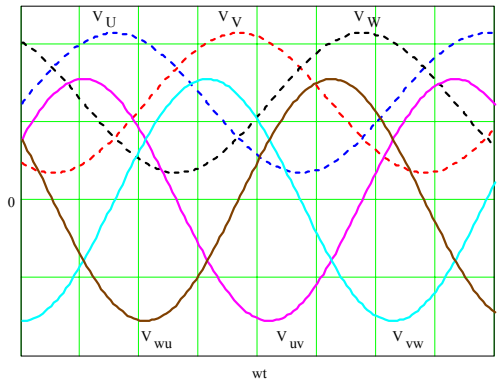

Fig. 4 Three-Phase Boost Inverter's Main Waveforms

The output voltage is the same in the three phases but with 120° delay between them. The signal is composed of a DC signal plus a sinusoidal waveform, as it is presented in (1).

$$V_U = V_{DC} + \sqrt{2} \cdot V_0 \cdot \sin(\omega t)$$
$$V_V = V_{DC} + \sqrt{2} \cdot V_0 \cdot \sin(\omega t - 120°) \quad (1)$$
$$V_W = V_{DC} + \sqrt{2} \cdot V_0 \cdot \sin(\omega t - 240°)$$

The initial specifications of this project and the main results can be observed in Table 1 and

Table 2 respectively. It is worth noting to design the components, the converter was considered to be operating using the PWM (Pulse Width Modulation) technique.

Table 1 – Initial Specifications

$V_{in} = 48Vdc$	Input Nominal Voltage
$V_{U,V,W} = 127V$	Phase Voltage
$V_{UV,VW,WU} = 220V$	Line Voltage
$P_{out} = 3cv\ (2208W)$	Output Nominal Power
$\Delta Ii = 20\%$	Input Current Ripple
$\Delta Vo = 5\%$	Output Voltage Ripple
$F_s = 20kHz$ to $50\ kHz$	Switching Frequency

Table 2 – Main Results

$Lin = 130\mu H$	Input Inductor
$Cout = 20\mu F$	Output Capacitor
$Iin\_max = 83A$	Maximum Input Current
$Iin\_min = -30A$	Minimum Input Current

III. CONTROL

The siding mode control has been presented as a good alternative to control switching power converters [9-10]. Some advantages over classic controllers are the stability on supply and load variations, robustness, good dynamic response and simple implementation.

The posterior analysis and control block diagram are designed for a single phase, due to the three phases are symmetrical. Fig. 5 shows the control block diagram. In this figure it is worth noting there is no electrical current reference because this variable is not directly controlled. The control methodology uses a hysteresis based on the error variables, where the voltage error is not enough to control the power converter, so the input current ripple helps the control to impose the correct switch during the converter operation. It is important to observe that just the input current is used on the control and its rms value will depend on the load applied to the system.

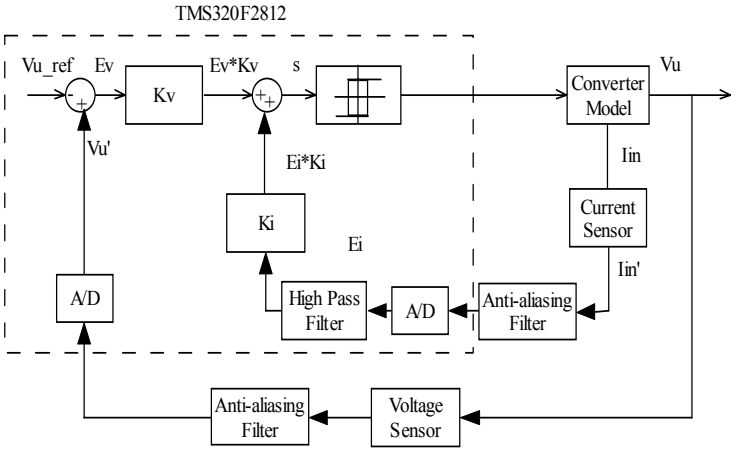

Fig. 5 Control Block Diagram

There are two different stages in the sliding mode control:

- Non-Sliding Mode or reaching mode, where the variables are reaching the sliding surface;
- Sliding Mode, where the variables are on the surface and sliding to the equilibrium point.

So, the control should be attractive enough to assure all the space states reach the sliding surface in a finite time.

A. Control Design Methodology

The first stage to design the sliding mode control is to find the boost state-space model. The load of the converter is considered linear. In the first stage, Q_1 is open and Q_2 is closed and in the second stage, Q_2 is open and Q_1 is closed.

The state-space modeling of the equivalent circuit with state variables i_L (input inductor current) and V_C (output capacitor voltage) is given by (2).

$$\begin{bmatrix} \frac{dV_c}{dt} \\ \frac{di_L}{dt} \end{bmatrix} = \begin{bmatrix} \frac{-1}{RC} & \frac{1}{C} \\ \frac{-1}{L} & 0 \end{bmatrix} \cdot \begin{bmatrix} V_C \\ i_L \end{bmatrix} + \begin{bmatrix} \frac{-i_L}{C} \\ \frac{V_C}{L} \end{bmatrix} \cdot \gamma + \begin{bmatrix} 0 \\ \frac{V_{in}}{L} \end{bmatrix} \quad (2)$$

Where:

$$\gamma = \begin{cases} 1 & when\ Q_1\ on\ /\ Q_2\ off \\ 0 & when\ Q_1\ off\ /\ Q_2\ on \end{cases}$$

$V_C = V_U = V_V = V_W$ = Output Voltage
$I_L = I_U = I_V = I_W$ = Input Currente
C = $C_U = C_V = C_W$ = Output Capacitor
L = $L_U = L_V = L_W$ = Input Inductor
R = Load

It is important to note the equations above can be represented by (3).

$$\dot{x} = A \cdot x + B \cdot \gamma + C \quad (3)$$

A switching surface s(x)=0 represents a desired system dynamics, which has a lower order than the given converter model. The sliding surface equation in the state space is expressed by a linear combination of the state variable errors and it can be observed in (4).

$$s(V_C, i_L) = K_v \cdot E_V + K_i \cdot E_i \quad (4)$$

Where:

$$\begin{aligned} E_V &= V_C - V_{C\_ref} \\ E_i &= i_L - i_{L\_ref} \end{aligned} \quad (5)$$

Replacing (5) in (3), the equation can be redefined by (6).

$$\dot{\varepsilon} = A \cdot \varepsilon + B \cdot \gamma + D \quad (6)$$

Where:

$$D = \begin{bmatrix} \frac{i_{L\_ref}}{C} & \frac{-V_{C\_ref}}{RC} \\ \frac{V_{in}}{L} & \frac{-V_{C\_ref}}{L} \end{bmatrix}$$

The existence condition of the sliding mode requires that all the trajectories near the surface are directed towards it.
In mathematical terms, this condition is expressed by (7).

$$\begin{aligned} s(x) > 0 &\rightarrow \dot{s}(x) < 0 \\ s(x) < 0 &\rightarrow \dot{s}(x) > 0 \end{aligned} \quad (7)$$

The status of the switching is related to the value of s(x).

$$\gamma = \begin{cases} 0 \rightarrow s > 0 \\ 1 \rightarrow s < 0 \end{cases} \quad (8)$$

Due to the information in (2), (7) and (8), the existence conditions can be expressed by (9) and (10).

$$K_V \cdot \left(\frac{i_{L\_ref}}{C} - \frac{V_{C\_ref}}{RC} \right) + K_i \cdot \left(\frac{V_{in}}{L} - \frac{V_{C\_ref}}{L} \right) < 0 \quad (9)$$

$$K_V \cdot \left(\frac{-V_{C\_ref}}{RC} \right) + K_i \cdot \left(\frac{V_{in}}{L} \right) > 0 \quad (10)$$

A sufficient condition is that the coefficients K_V and K_i be nonnegative.

B. Switching Frequency

The state trajectories are directed toward the sliding surface and move exactly along it, only if the switching frequency is infinite. It is not possible in practical systems, so a typical control circuit features a hysteresis comparator with width 2δ is implemented as it can be observed in Fig. 6.

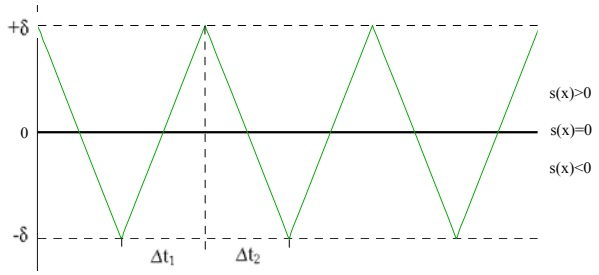

Fig. 6 S(x) Behavior

The switching frequency is shown in (11), where Δt_1 is the conduction time of the switch Q_1 and Δt_2 is the conduction time of the switch Q_2.

$$fs = \frac{1}{\Delta t_1 + \Delta t_2} \quad (11)$$

The times quantities for Δt_1 and Δt_2 can be found using (12).

$$\dot{s} = \frac{\Delta s}{\Delta t} \quad (12)$$

Using (12) it is possible to find an equation to represent Δt_1 and Δt_2.

$$\Delta t_1 = \frac{2\delta}{K_V \cdot \left(\frac{-V_{C\_ref}}{RC}\right) + K_i \cdot \left(\frac{V_{in}}{L}\right)} \quad (13)$$

$$\Delta t_2 = \frac{-2\delta}{K_V \cdot \left(\frac{i_{L\_ref}}{C} - \frac{V_{C\_ref}}{RC}\right) + K_i \cdot \left(\frac{V_{in}}{L} - \frac{V_{C\_ref}}{L}\right)} \quad (14)$$

The maximum switching frequency is obtained when the converter is operating without load (i_{Lref}=0 and R= ∞) and it can be obtained replacing (13) and (14) in (11).

$$f_{s\_\max} = \frac{K_i \cdot V_{in}}{2 \cdot \delta \cdot L}\left(1 - \frac{V_{in}}{V_{C\_ref\,\max}}\right) \quad (15)$$

C. Specifications and Results

In Table 3 are the necessary specifications to calculate de sliding mode gains.

Table 3 – Control Specifications

V_{in} = 48Vdc	Input Nominal Voltage
fsmax=50 kHz	Maximum Frequency
Vcref_max=429.6V	Maximum Output Voltage
2δ=0.6	Amount of Hysteresis
R=55.3Ω	Load

The sliding mode current gain (K_i) can be obtained using (15).

$$K_i = 0,091 \quad (16)$$

And equations (9) and (10) are used to find the sliding mode voltage gain (K_V).

$$K_V < 0,08 \quad \textit{and} \quad K_V < 0,086 \quad (17)$$

D. Flowchart

A flowchart was designed to help and make easier the source code creation.

The main code is just to configure all the peripherals, clocks and create the variables used in the control. The software has an ADC interrupt after each ADC conversion. In the interrupt routine, the sliding mode control is implemented and the switches pulses are created. If an error signal from the drivers reaches the DSC, the external interrupt occurs and all the switches are opened. Fig. 7 shows the main flowchart. The ADC and Xint interrupts flowcharts can be observed in Fig. 8.

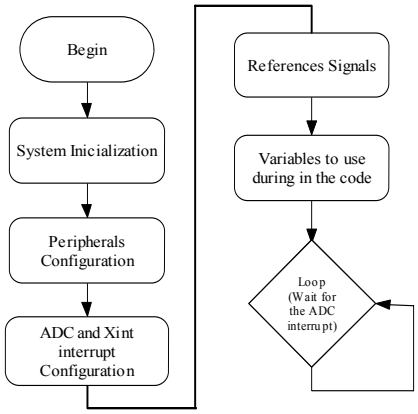

Fig. 7 Main Flowchart

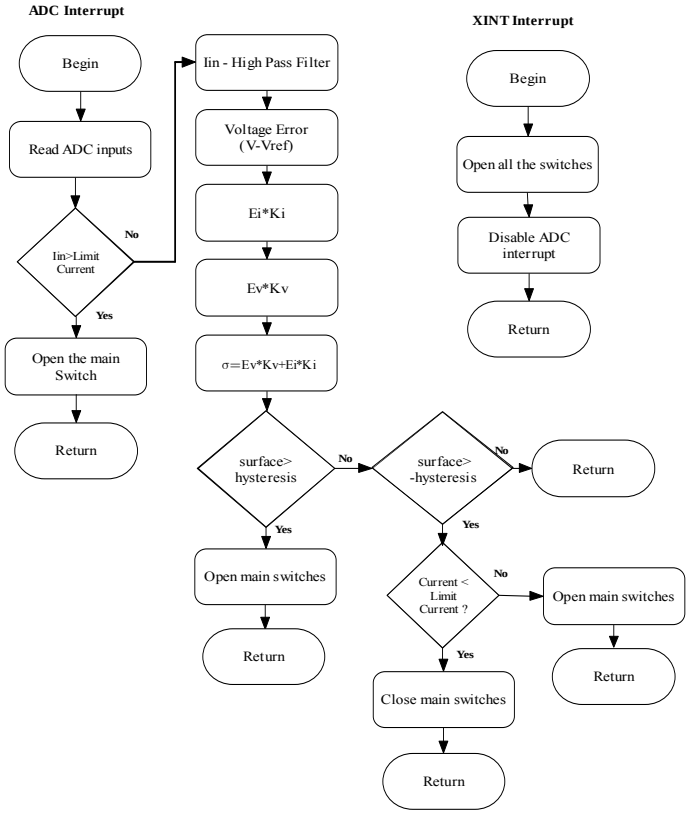

Fig. 8 ADC and Xint Interrupt

IV. EXPERIMENTAL RESULTS

A. Simulation Results

In order to validate the theoretical analysis, the digital sliding mode controlled three-phase boost inverter was simulated using the package *Simulink* from the software *Matlab*. Fig. 9 shows the output voltages using 3.33ns sample period.

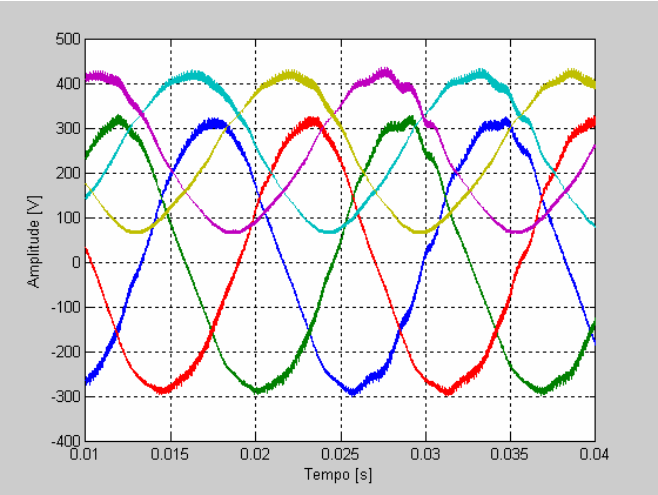

Fig. 9 Output Voltages

In Fig. 10 is shown the input current in one of the phases. The current in other phases is similar, just with a 120° delay.

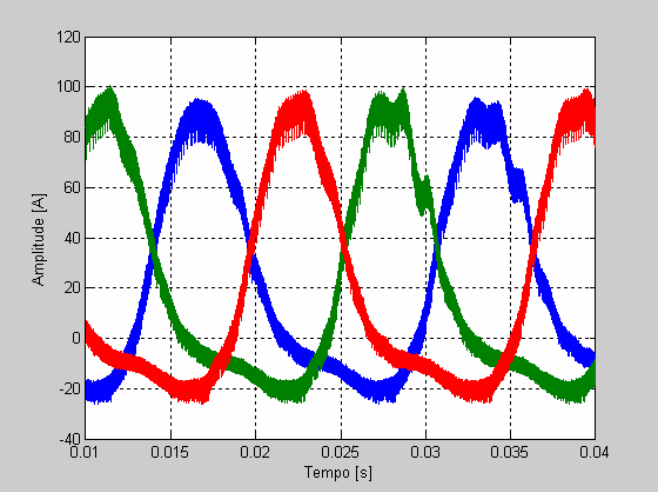

Fig. 10 Input Current

B. Prototype

After to design the control and validate its efficiency by simulations, a prototype was build to acquire experimental results.

The control was digitally implemented using a DSC and some signal conditioning was necessary to assure good accuracy in the analogical to digital conversion. Fig. 11 shows a converter block diagram.

The voltage sensors used in this prototype were resistive dividers. They were chosen due to their costs and no isolation requirements. Due to the reference used in the control and the structure itself, the sensors used to measure the input currents were isolated Hall-Effect sensors.

The anti-aliasing filters avoid the spectrum superposition on sampled systems. The cut-off frequency of the anti-aliasing filter of the voltage feedback signal is approximately 120Hz and the current feedback signal is approximately 150kHz.

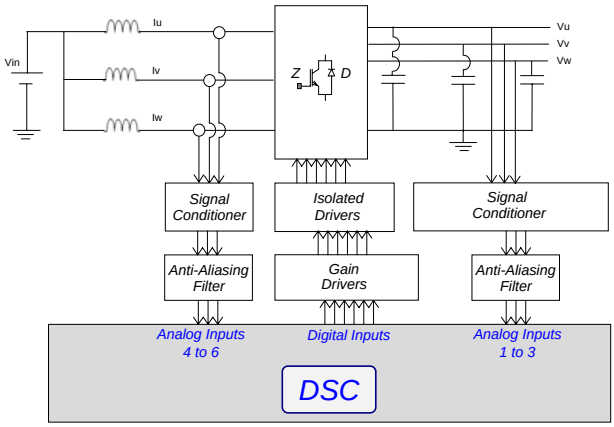

Fig. 11 Converter Block Diagram

The developed software was created to calculate the variables involved in the control technique at 300 kHz using the Analog to Digital Interruption. The current sample is filtered using an IIR (Infinite Impulse Response) digital filter to keep just the electrical current ripple. The voltage sample is compared with the current voltage reference vector position and reserved to the later calculations. The voltage reference vector was created using 380 positions and by this reason, its index is incremented each 13 interruptions.

Using the voltage error and the filtered current, the sliding mode gains are applied as presented in Fig. 5, and sent to the hysteresis comparator. Using the output hysteresis comparator, the states switches are updated.

Some special features were created to allow the corrected operation of the system. A soft-start procedure was implemented to boost the output voltage for 3 intermediate levels using a ladder profile before applying the nominal voltages references in order to eliminate electrical current peaks. An electrical current limitation is applied each cycle, avoiding current peaks higher than maximum under nominal operation. During the software development, special routines were implemented to allow the developer to stop the processor being sure the main switches were opened and will not cause any damage to the system.

The whole encoding were done using C language and the libraries available in the processor's manufacturer website. In order to be sure the compiler were not using too much assembly for each C language encoded line, the generated assembly code was verified for the whole control technique related code.

C. Experimental Results

Experimental results were obtained using the prototype specified in Table 1.

The results presented in this section were obtained using a full load.

Fig. 12 shows the three output voltage and Fig. 13 shows the line voltages.

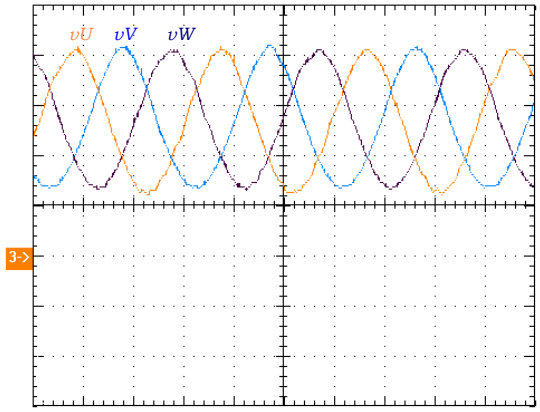

Fig. 12 Output Voltage (*vU – vV – vW*: 100V/div, 5ms)

Fig. 15 – Inductor Current (10A/div, 2.5ms)

Fig. 13 Line Voltages (*vUV , vVW, vWU*: 100V/div, 5ms)

Fig. 16 Line Voltages – 45Hz (*vUV – vVW – vWU*: 100V, 5ms)

In Fig. 14 can be observed the motor's current.

Fig. 14 Motor's Current (*iUV – iVW – iWU*: 2A/div, 10ms)

Fig. 17 Line Voltages – 75Hz (*vUV – vVW – vWU*: 100V, 2.5ms)

Other important waveform that should be observed is the inductor current that is presented in Fig. 15.

To assure the control technique, two different frequencies in voltage reference signal were applied. The Fig. 16 and Fig. 17 present the output voltage with different frequencies.

It is important to note that in the start of the motors, the current is very high. So, to minimize that, the algorithm was developed to purpose a soft start to the motor where two different DC levels are applied to the converter output and after that the AC signal starts with small amplitude and it should getting high until the nominal amplitude. The soft start of the motor is presented in Fig. 18. Fig. 19 shows de prototype implemented.

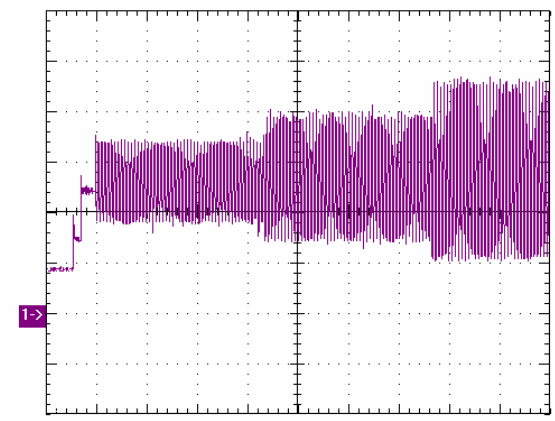

Fig. 18 – Soft Start of the Motor (100V/div, 250ms)

Fig. 19 – Prototype of inverter

V. CONCLUSION

This paper presented a Digital Sliding Mode Controlled Three-Phase Boost Inverter and its theoretical analysis with the main equations of its control.

In order to validate the theoretical analysis, the circuit was simulated and implemented as a 2.2kW prototype. The experimental output voltages, input currents and switching behavior waveforms closely matched the theoretical ones. One advantage of digital sliding mode control is its easy code creation and facility to adjust the practical gains. On the other hand, by the reason that this control technique is based on hysteresis, the processor should be very fast to be able to process a great number of samples and compare it with the hysteresis. In practical experiments the authors conclude that is necessary a sampling frequency at least 6 times greater that the maximum switching frequency to obtain a good control response.

The nominal results were acquired with a 90Vdc input voltage. It was necessary because it is not possible to get the nominal power with 48Vdc, due to the non linear characteristic of the boost inverter, mainly for high gains.

ACKNOWLEDGEMENT

The authors gratefully acknowledge the donation of the EzDSP2812 development kit from *Texas Instruments*, the output capacitors from *WEG Industry – Brazil* and the input toroidal inductors from *Magmatech – Brazil*. Santa Catarina State University financial support with a scholarship is also gratefully acknowledged.

REFERENCES

[1] M. Mezaroba, P. S. G. Giacomini, J. S. Scholtz. "Conversor Elevador/Abaixador com Comutação Suave ZVS PWM e Grampeamento Ativo". *INDUSCON – Conferência Internacional de Aplicações Industriais*. Bahia – Brazil, 2006.

[2] V. I. Utkin, "Sliding Modes in Control Optimization". Berlin 1992, ISBN 3-540-53516-0.

[3] U. Itkin, "Sliding Modes and Their Application in Variable Structure Systems". MIR Publishers, Moscow, 1974.

[4] R. Venkataramanan, A. Sabanovic, S. Cuk. "Sliding Mode Contro of DC to DC Converters". *Power Electronic Group, CalTech*, 1986.

[5] P. Mattavelli, L. Rossetto, G. Spiazzi, "General - Purpose Sliding - Mode Controller for DC/DC Converter Applications". 1993. *PESC – Power Electronics Specialist Conference. 25th Annual IEEE,* pp. 609-615.

[6] R. O. Cáceres, I. Barbi, "A Boost DC-AC Converter: Analysis design, and Experimentation." *IEEE Transactions on Power Electronics*, 1999, pp. 134-140.

[7] R. Cáceres, I. Barbi, "Sliding Mode Controller for the Boost Inverter". 1996, *CIEP – International Power Electronics Congress*, pp. 247-252.

[8] S.A. Bock, J.R. Pinheiro, H, Gründling, H.L. Hey, H. Pinheiro. "Existence and Stability of Sliding Modes in Bi-directional DC - DC Converters". 2001, *PESC – Power Electronics Specialist Conference, 32nd Annual IEEE*, pp. 1283 – 1288.

[9] H. Sira-Ramirez. "Sliding Mode Control for AC to DC Converters". *CBA – Congresso Brasileiro de Automática* 1988. pp. 21-26.

[10] H. Pinheiro, A. Martins, J. Pinheiro. "Single Phase Voltage Inverters Controlled by Sliding Mode". *CBA – Congresso Brasileiro de Automática* 1994. pp. 1177-1182.

[11] J.Y. Hung, W. Gao, J. C. Hung, "Variable Structure Control: A Survey". *IEEE Transaction on Industry Electronics*, 1993, pp. 02-21.

[12] W. M. Pastorello Filho, N. Batistela, A. J. Perin. "Controle por Modos Deslizantes Aplicado a Conversores Estáticos de Potência". *SEP – Seminário de Eletrônica de Potência* - UFSC 1995.

[13] R. O. Cáceres I. Barbi, "Família de Conversores CC – CA, Derivados dos Conversores CC – CC Fundamentais.". Tese de Doutorado. UFSC, 1997.

[14] I. E. Colling, "Conversores CA – CC Monofásicos e Trifásicos Reversíveis com Elevado Fator de Potência". Tese de Doutorado. UFSC, 2000.